

Insulator–metal phase transition and superconductivity in $\text{Ba}_{1-x}\text{K}_x\text{BiO}_3$

N. V. Anshukova and A. I. Golovashkin

P. N. Lebedev Institute of Physics, Russian Academy of Sciences, 117924 Moscow, Russia

L. I. Ivanova, O. T. Malyuchkov, and A. P. Rusakov

Moscow Institute of Steel and Alloys

(Submitted 15 May 1995)

Zh. Éksp. Teor. Fiz. **108**, 2132–2146 (December 1995)

A physical model of the electronic structure, mechanisms of the insulator–metal and metal–superconductor phase transitions in $\text{Ba}_{1-x}\text{K}_x\text{BiO}_3$ based on experimental studies of specific heat, thermal expansion coefficients, and magnetic properties has been proposed. All the observed anomalies of physical properties of $\text{Ba}_{1-x}\text{K}_x\text{BiO}_3$ have been interpreted in terms of this model. © 1995 American Institute of Physics.

1. INTRODUCTION

The compound $\text{Ba}_{1-x}\text{K}_x\text{BiO}_3$ (BKBO) is an interesting material, which displays high- T_c superconductivity (HTSC) with a critical temperature $T_c > 30$ K, does not contain copper, and transforms to an insulator phase in a mysterious manner at a definite potassium content (concentrational phase transition). Compounds of this kind demonstrate in both normal and superconducting states several anomalous properties, which can be hardly described in terms of existing concepts. For example, in high-quality superconducting BKBO samples, an anomalous upward curvature of the upper critical magnetic field H_{c2} plotted against temperature in a range down to almost zero was detected.^{1–3}

The group of BKBO compounds presents a specific case of a wider family of bismuth-oxide materials, which also includes layered compounds with a structure similar to that of La_2CuO_4 . For example, when Ba_2BiO_4 is doped with potassium and lead, a layered material with T_c a factor of two higher than that of the cubic structure is produced.⁴

The traditional explanation of the transition to the insulator phase in BKBO compounds is unequal sharing of electrons among Bi atoms: $2\text{Bi}^{+4} \rightarrow \text{Bi}^{+3} + \text{Bi}^{+5}$. The large difference between radii of Bi^{+3} and Bi^{+5} ions leads to a considerable difference between dimensions of surrounding oxygen octahedrons. Alternation of octahedrons of different dimensions (such a structure is traditionally called a “breathing mode”⁵) doubles the lattice constant, and a dielectric gap is opened on the Fermi level. But direct electron-microscopic measurements with atomic resolution did not detect oxygen octahedrons with significantly different dimensions in $\text{Ba}_{1-x}\text{K}_x\text{BiO}_3$ for $x < 0.1$ (Ref. 6). At the same time, the insulating gap for $x > 0.1$ is practically identical to that at $x = 0$ (Ref. 7). Thus we have to accept that the “breathing mode” concept contradicts experimental data. The problem of the BKBO insulator phase is not resolved by the model of partial sharing of charge among bismuth ions which assumes that bismuth ions exist in two states, $\text{Bi}^{+4+\delta}$ and $\text{Bi}^{+4-\delta}$, where $0 < \delta < 1$ (Ref. 8). In this case, BKBO would contain local magnetic moments because Bi^{+4} ions are magnetic. Accurate muon-scattering experiments (muon spin reso-

nance, μSR), however, did not detect any local magnetic moments of bismuth ions in BKBO.^{9,10}

The anomalous curvature of the $H_{c2}(T)$ curve in superconducting BKBO samples should be also accounted for. The function $H_{c2}(T)$ was measured by different authors in high-quality samples, including single crystals.^{1–3} This anomaly cannot be due to contributions of different superconducting phases or impurities. In the mean-field approximation (within the BCS model) such a shape of the $H_{c2}(T)$ curve can be obtained only if $\lambda \gg 1$ (Ref. 11), where λ is the electron-phonon coupling constant. But various experiments with BKBO yield $\lambda \leq 1$.^{1,12} Therefore the BKBO superconductivity cannot be described by the standard BCS model.

Thus the topics of the insulator phase, ordering of the electron density, insulator–metal and metal–superconductor phase transitions in BKBO present a considerable challenge and demand further research.

The paper proposes a physical model of the electronic structure compatible with insulator–metal and metal–superconductor transitions in BKBO and based on experimental studies of specific heat, magnetic properties,¹ and thermal expansion.¹³ Some preliminary results of our studies were published earlier.^{14–17}

2. EXPERIMENT

We have developed techniques for synthesizing high-quality BKBO samples with a large volume of the Meissner phase ($> 50\%$) near T_c .^{18,19} Polycrystalline samples were synthesized by the nitrate method, which is a modification of the two-stage technique described in Ref. 20. Single crystals were grown using a modified version of the electrochemical technique described in Refs. 21 and 22. An important point is that the optimum times of synthesis and annealing of a polycrystalline sample are functions of its weight. Unlike Refs. 21 and 22, single crystals were synthesized in a pure nitrogen atmosphere, i.e., oxygen was not used during any synthesis step. We have discovered that there are narrow ranges of temperature (around 320 °C) and melting stock composition in which single-phase, high-quality samples with a sharp diamagnetic transition at $T \approx 30$ K and a large volume of the Meissner phase are produced. The large volume of the

Meissner phase near T_c allows reliable measurements of the specific heat jump at a high magnetic field.¹ Besides, the constant volume of the Meissner phase in a wide temperature range is vitally important in interpreting the anomalous shape of the $H_{c2}(T)$ curve observed in BKBO.

The phase diagram of the Ba–K–Bi–O system has been investigated. As Pei *et al.*²⁰ found earlier, for $x < 0.3$ the samples are single-phase insulators. For $0.3 < x < 0.6$ single-phase metal samples with superconducting properties are synthesized. At a higher potassium content samples containing several phases are produced.

The X-ray and neutron diffraction, optical spectra, resistivity under magnetic field, elastic parameters, magnetic susceptibility, and temperature dependence of the resistivity of the samples have been measured. The maximum critical temperature $T_c \cong 30$ K was detected in metal samples with x close to the insulator–metal transition. The critical temperature drops with x and is about 16 K at $x = 0.55$. The lattice cell also decreases with x . According to X-ray and neutron scattering data, no notable density jump is detected at the insulator–metal transition ($x \cong 0.3$). The crystal symmetry also does not change at the transition point.²³

In the range $0.1 < x < 0.6$ the structure of BKBO is cubic. Raman scattering data, however, indicate that there are local distortions of the cubic symmetry in our samples,²⁴ therefore it is more appropriate to consider a pseudo-cubic syngony. The band gap at a small x is about 2 eV.

The magnetic susceptibility χ of the samples was measured in a temperature range of 2–300 K. No traces of paramagnetic impurities were detected in both insulator samples and in metallic samples in the normal state. In the superconducting state, a large Meissner effect (50–70% of the ideal value) is observed in a narrow temperature range (< 5 K) near T_c in both polycrystalline and single-crystal samples. The susceptibility was measured in a magnetic field of $H = 2$ Oe using a vibrational magnetometer. Measurements of the temperature dependence of the sample resistivity for $x > 0.3$ demonstrated the metallic conductivity. In $\text{Ba}_{0.6}\text{K}_{0.4}\text{BiO}_3$ single crystals, the ratio of resistivities at 300 K and 40 K was 2–3.

The temperature dependence of the specific heat, $C(T)$, in the samples with a strong Meissner effect was measured in a magnetic field of up to 200 kOe.¹ Given the high quality of the samples, the specific heat jump at T_c could be measured and $H_{c2}(T)$ curve could be plotted in a wide temperature range.

Figure 1 shows a curve of $H_{c2}(T)$ plotted using measurement data of the specific heat and magnetic susceptibility. For comparison experimental data from Ref. 2 and 3 derived from resistivity measurements under a field of up to 32 T are plotted in the same graph. One can see that measurements by different authors performed on high-quality samples are in a close agreement. No sign of the temperature derivative of H_{c2} dropping to zero at low temperatures, as predicted by the BCS theory, can be seen, whereas the paramagnetic limit $H_p \cong 1.84T_c$, according to BCS, is 55 T. At low temperatures, the measured values of H_{c2} are several times higher than the BCS prediction.²⁵

The electron-phonon coupling constant ($\lambda = 0.9$) was de-

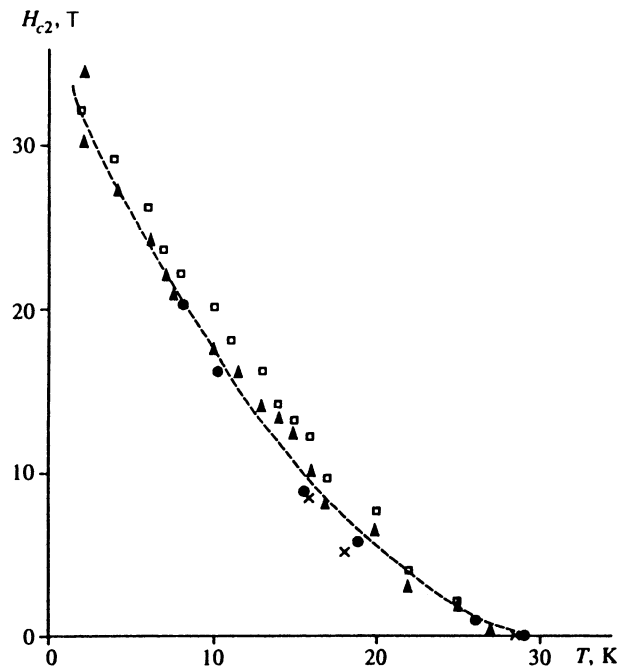


FIG. 1. Upper critical magnetic field H_{c2} versus temperature in $\text{Ba}_{0.6}\text{K}_{0.4}\text{BiO}_3$: (●) data derived from specific heat measurements; (×) data derived from magnetic susceptibility; (□) and (▲) resistivity measurements from Ref. 2 and 3, respectively.

rived from the coefficient γ at the linear term of the specific heat as a function of temperature. The procedure for determining γ in the normal BKBO state was the following: at each magnetic field H a point γ_H on the ordinate axis of the C/T versus T^2 plot defined by crossing with an experimental curve was determined. Then the curve of γ_H versus H was plotted and extrapolated to the high-field region, where the function saturated.

The thermal expansion coefficient α of BKBO samples with different potassium contents in both insulator and metallic phases was measured.¹³ We discovered that for $x < 0.4$ and low temperatures, α is negative (Fig. 2), i.e., at low temperatures BKBO samples contract when heated. The maximum contraction was observed in samples with small x ,

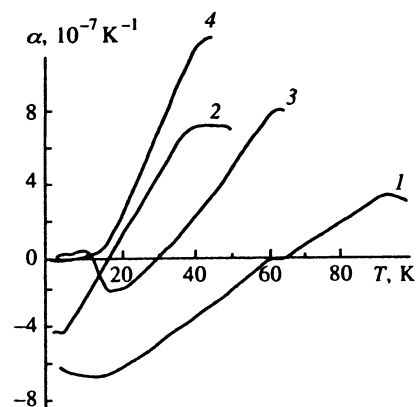


FIG. 2. Thermal expansion coefficient α versus temperature in $\text{Ba}_{1-x}\text{K}_x\text{BiO}_3$: 1) $x = 0.13$; 2) $x = 0.27$; 3) $x = 0.4$; 4) $x = 0.55$.

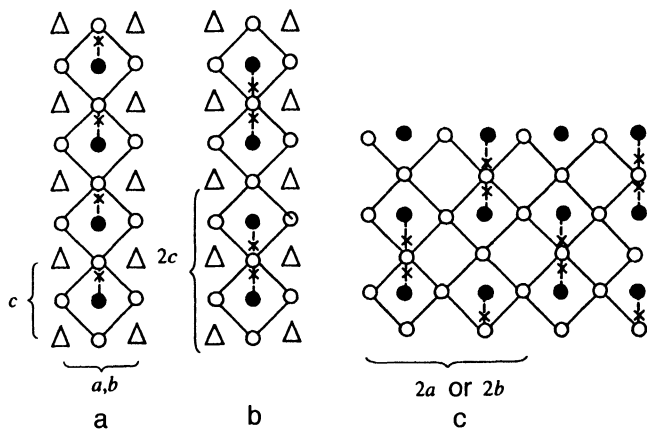


FIG. 3. Electronic structure of $\text{Ba}_{1-x}\text{K}_x\text{BiO}_3$ at small x (<0.3): (●) Bi^{+3} ion; (○) O^{-2} ion; (△) Ba^{+2} or K^{+1} ion; (×) localized hole on a Bi–O bond; a) in-phase ordering of localized holes along c -axis; b) counterphase ordering of holes along c -axis leading to doubling of lattice cell in this direction; c) doubling of cell dimensions along a and b -axes due to counterphase ordering of localized holes.

and the temperature range in which their α is negative extends to 60 K. At a higher potassium content, the absolute value of α is smaller and the temperature range in which it is negative is narrower. But even in metallic samples with $x=0.4$ the thermal coefficient α is negative in a considerable temperature range of up to 15 K. Thus the samples with the maximum T_c have a negative thermal expansion coefficient in some temperature range. At $x=0.5$ the samples have a positive thermal expansion coefficient throughout the studied temperature range. The curve of the temperature at which thermal contraction is replaced by thermal expansion plotted against potassium concentration displays a feature near the insulator–metal phase transition.

3. A MODEL OF ELECTRONIC STRUCTURE AND INSULATOR–METAL PHASE TRANSITION

The experimental data cannot be accounted for in terms of existing models of the BKBO electronic structure. Therefore we propose a model of the BKBO structure, which allows us to explain both the insulator–metal transition and other unusual experimental results.

At small x ($x < 0.3$) the upper valence band of BKBO is largely formed by the $\text{O}(2p)$ states, and holes of this band have the symmetry of the $\text{O}(2p)$ state.^{26,27} Given the combination of all experimental data, we assume that the valence band of undoped BaBiO_3 is described by a partially covalent formula $\text{Ba}^{+2}\text{Bi}^{+3}\text{O}_2^{-2}\text{O}^{-1}$, i.e., a localized hole is near one of apical ions of the oxygen octahedron. To be exact, this hole is placed on a Bi–O bond (Fig. 3a), and its position depends on the admixture of the $\text{Bi}(6s)$ states to $\text{O}(2p)$ on the Fermi level. We shall denote the $\text{Bi}^{+3}\text{O}^{-2}$ bond with a localized hole on it as $\text{Bi}^{+3}\text{O}^{-1}$. For each oxygen octahedron with a Bi^{+3} ion inside, there is only one bond with a hole localized on it. These bonds can be ordered along the c -axis to form the $\text{Bi}^{+3}\text{O}^{-1}\text{Bi}^{+3}\text{O}^{-1}$ chain, i.e., to order the localized holes in phase (Fig. 3a). If these bonds with localized holes are directed towards each other, the

$\text{Bi}^{+3}\text{O}^0\text{Bi}^{+3}\text{O}^{-2}\text{Bi}^{+3}\text{O}^0$ chains are formed on the c -axis, i.e., the localized holes are ordered in counterphase and the lattice period along this axis is doubled (Fig. 3b). The respective doubling of the lattice period along other two crystal axes, a and b , is shown in Fig. 3c. In terms of tight binding, this means that there is only one partly covalent bond among ionic bonds in each oxygen octahedron around a Bi^{+3} ion. Thus the counterphase ordering of partly covalent bonds along crystal axes results in the doubling of the lattice cell, hence an insulating gap E_g on the Fermi level appears. Experimental data indicate that at small x we have $E_g \approx 2$ eV.^{28,29} At a potassium doping of up to $x \approx 0.3$ the energy gap E_g is slightly smaller, but in general the electronic structure is the same.

Thus in the proposed model of the electronic structure of BKBO, oxygen ions at two opposite apices of the octahedron around Bi have different valences (i.e., apical oxygen ions along the c -axis have different charges). In neighboring oxygen octahedra aligned with the a - and b -axes, the valence of apical oxygen ions alternates similarly, but in counterphase. In terms of energy bands, a commensurable charge density wave (CDW) with antinodes at apical oxygen atoms is formed. A periodic Coulomb potential is connected with this CDW which leads to dielectrization of an electronic spectrum on the Fermi surface. Therefore, BKBO is an insulator (not a metal) at low doping levels. This model does not demand any “breathing mode.” Note that this model predicts two different Bi–O separations (Bi^{+3}O^0 and $\text{Bi}^{+3}\text{O}^{-2}$) because of the difference between O^0 and O^{-2} radii. The high-resolution electron-microscope pattern indeed reveals a small modulation of separations between bismuth and oxygen atoms.⁶

We should also note that for $x < 0.1$ the BKBO lattice is also distorted (tilting) because of the difference between oxygen ions dimensions. For simplicity, this effect is not shown in Fig. 3.

If some Bi atoms are substituted with Pb, the patterns shown in Fig. 3 can be also applied to the $\text{Bi}_{1-x}\text{K}_x\text{Pb}_{1-y}\text{Bi}_y\text{O}_3$ compound.

At a heavier potassium doping of BKBO, light charge carriers screening the Coulomb potential generated by ordered heavy holes are introduced, and this potential and localization degree are decreased. For $x \geq 0.3$ the material has metallic conductivity (concentrational insulator–metal phase transition).

The pattern of holes proposed for BKBO localized near apical oxygen ions and their ordering resulting in an insulating gap on the Fermi level can also be applied to copper-oxide superconductors after some modifications. Whereas in BKBO the oxygen octahedra are connected to each other, in copper-oxide superconductors they are separated along the c -axis. In La_2CuO_4 they are separated by two LaO layers (Fig. 4b). But in La_2CuO_4 , just as in BKBO (Fig. 4a), there is one partly covalent bond (a localized hole) per each oxygen octahedron. Counterphase ordering of these hole bonds leads to formation of CDW, i.e., an alternating valence of apical oxygen ions along the c -axis. A phase shift similar to BKBO takes place in the ordering of such bonds along the a and b -axes (Fig. 3c). The charge density wave leads to an

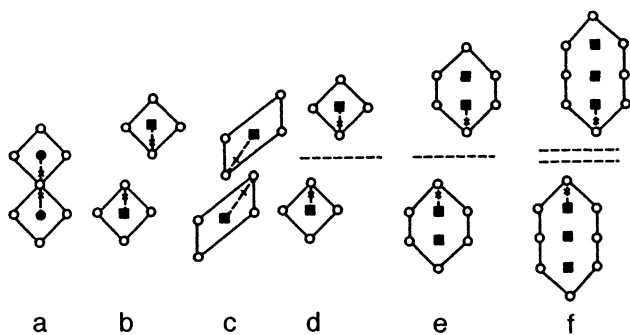


FIG. 4. Localization of heavy holes and their counterphase ordering in copper- and bismuth-oxide superconductors: (●) bismuth ion; (■) copper ion; (○) oxygen ion; (×) localized heavy hole on Cu–O and Bi–O apical bonds; dashed lines shows TlO layers or CuO chains (for clarity, other ions are not shown). Pairs of oxygen polyhedra (for BaBiO₃ a pair of oxygen octahedra) with two hole bonds directed oppositely are shown for the following materials: a) Ba_{1-x}K_xBiO₃; b) La_{2-x}Sr_xCuO₄; c) Nd_{2-x}Ce_xCuO₄; d) TlBa₂CuO₅; e) TlBa₂CaCu₂O₇ or YBa₂Cu₃O₇; f) Bi₂Sr₂Ca₂Cu₃O₁₀.

energy gap on the Fermi level. When La₂CuO₄ is doped with strontium (La_{2-x}Sr_xCuO₄, LSCO), it becomes a metal, just as BKBO doped with potassium.

The separation of oxygen octahedra along the *c*-axis in La₂CuO₄ means that an oxygen ion with a localized hole on it has a charge of -1 instead of 0 in BKBO where the octahedra have a common oxygen atom.

An important point is that in copper-oxide superconductors a hole is also localized on an apical bond, in the case of La₂CuO₄ on the Cu–O bond. But whereas in BKBO the admixture of the bismuth states to the oxygen states on the Fermi level is only several percents,^{26,27} in La₂CuO₄ the admixture of the copper states is more than 30%. This means a notable shift of the hole towards the copper ion. Hence a simplified chemical formula of this compound can be expressed as La⁺³Cu^{+(1+δ)}O₃⁻²O₁^{-(1+δ)}, where $\delta \approx 0.4$. This results in an antiferromagnetic ordering in La₂CuO₄ and LSCO at small *x* with a localized magnetic moment at a copper ion of 0.4 of the Bohr magneton.³⁰ Since two apical oxygen ions are involved instead of one, as in BKBO, spin density waves are generated in these compounds in addition to CDW. Therefore it is more correct to interpret LSCO properties in terms of the partially covalent hole bond instead of the O⁻¹ ion. In this discussion, we use the term “O⁻¹ ion” for simplicity. The crystal structures of BKBO and LSCO are, no doubt, quite different that results in differences between some of their physical properties, but here we discuss only the common features of covalent bonds and their ordering in these compounds resulting in the CDW and insulating gap.

A similar pattern of hole bonds ordering can be detected in Nd_{2-x}Ce_xCuO₄. Note only that the Nd ion dimension larger than that of La leads to a displacement of apical oxygen ions and distortion of oxygen octahedra (Fig. 4c). At a higher content of cerium, *n*-type charge carriers are produced, and the material has metallic conductivity.

Additional atomic layers can exist between oxygen octahedra. For example, an additional TlO layer between octa-

hedra results in a structure like TlBa₂CuO₅ (Fig. 4d). The mechanism of covalent bonds ordering and generation of CDWs is similar to that in La₂CuO₄ (Fig. 4b).

When there are two CuO₂ layers in one cell, as in TlBa₂CaCu₂O₇ or YBa₂Cu₃O_{6+x}, the oxygen octahedron is replaced with a polyhedron with apical oxygen atoms, as shown in Fig. 4e. Like an octahedron, this polyhedron contains one hole bond. Ordering of these bonds results in CDW in the material. In this case, the chemical formula of CuBa₂Cu₂YCu₂O_{6+x} can be expressed as Cu^{+2x}Ba₂⁺²Y⁺³Cu⁺²Cu^{+(2+δ)}O_{5+x}⁻²O^{-(1+δ)}, where $\delta < 0.5$ for $x < 0.5$ (in the insulator phase).³⁰

In the case when an oxygen polyhedron contains *n* CuO₂ layers (for example, in Bi₂Sr₂Ca_{n-1}Cu_nO_{2n+4}), the oxygen polyhedron is extended along the *c*-axis (Fig. 4f for $n=3$), but, all the same, contains only one covalent bond with an apical oxygen ion. Several atomic layers instead of one can be placed between apical oxygen ions (for example, two BiO layers in Fig. 4f). This model can be obviously generalized for other oxide superconductors.

Thus we can see that there is a mechanism common for all oxide superconductors which leads to CDWs and an insulating gap at a low doping level. This mechanism is manifested most distinctly in BKBO. If neighboring oxygen octahedra have a common oxygen ion on the *c*-axis (Fig. 4a), an antiferroelectric ordering occurs. If apical oxygen ions of octahedra or polyhedra are separated along the *c*-axis (Fig. 4b–f), an antiferromagnetic ordering may occur concurrently with CDWs.

We have discussed the effect of hole localization on the symmetry of the BKBO structure. Now let us consider the effect of localized holes ordering on the electron spectrum. Figure 5 schematically shows the BKBO electron spectrum around the Fermi level E_F at various potassium doping levels. For $x < 0.3$ there is a gap E_g in the electron density of states $N(E)$ ($E_g \approx 2$ eV for $x \approx 0.1$). There are acceptor impurity levels near the Fermi level due to doping (Fig. 5a). These levels are at 0.2–0.4 eV above the valence band top³¹ and are responsible for a *p*-type semiconductor conductivity. At a higher doping level ($x \approx 0.3$) an impurity band overlapping with the valence band top is formed by these levels (Fig. 5b). At an even higher doping level ($x \approx 0.5$) the band edges are broadened, the bands overlap, and the material has an *n*-type conductivity (Fig. 5c). Thus the material is a *p*-type conductor in the range $x \approx 0.3$ –0.4, where the critical temperature T_c is maximum.

We should note that even at potassium doping with $x = 0.3$ –0.4 the conductivity of samples with oxygen deficiency may be *n*-type. Indeed, oxygen vacancies in BKBO are donors, thus holes are compensated, superconductivity is not observed, and samples have high resistivity. Oxygen can be ejected from BKBO quite easily because some atoms have a valence close to zero (Fig. 3). The situation is similar in other high- T_c superconductors doped by substituting their cations (La_{2-x}Sr_xCuO₄, etc.).

In our discussion, we assumed for simplicity that the effective mass of localized holes is much larger than that of free carriers and their mobility is negligible. But at higher

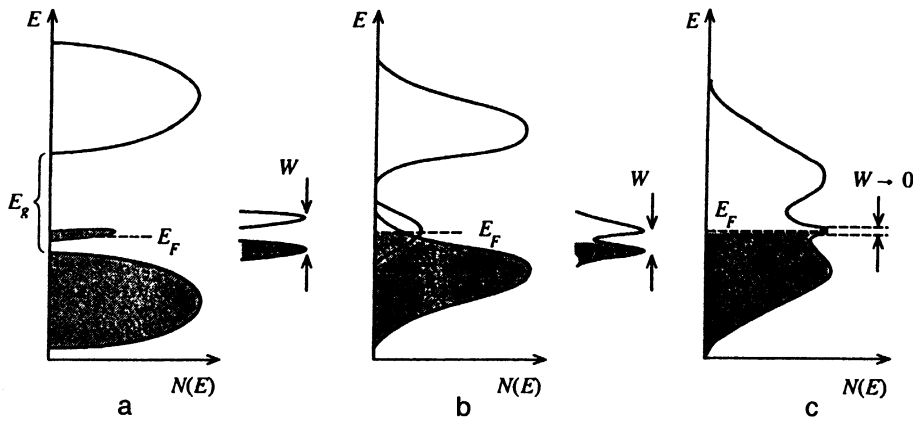


FIG. 5. Diagram of the $\text{Ba}_{1-x}\text{K}_x\text{BiO}_3$ electronic spectrum at different x : a) $x < 0.3$; b) $x \approx 0.3-0.4$; c) $x \geq 0.5$. Notations are given in the text.

temperatures or under a strong electric field, jumps of heavy holes between neighboring octahedra are possible, i.e., transitions from the ground to excited state across a band gap W . This will be discussed below.

We have demonstrated that CDWs emerge in BKBO owing to the ordering of holes localized on Bi-O apical bonds. We must note, however, that CDWs are doubly degenerated because there are two ways of distributing localized charges between two apical oxygen ions. Figure 6 shows two pat-

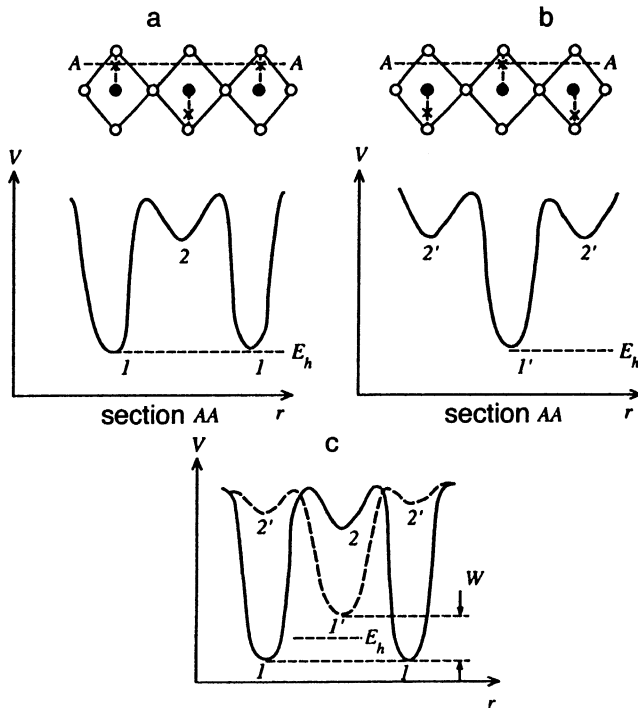


FIG. 6. Charge density waves and $V(r)$ curve in BKBO: (a and b) two modes of hole ordering along a -axis and respective curves of periodic potential $V(r)$; (c) $V(r)$ potential curves with degeneracy of CDWs lifted. The parameter W corresponds to the energy difference between (1) ground and (1') excited states of localized hole; E_h is the localized hole ground state energy with CDW degeneracy. Symbols denoting atoms are the same as in Fig. 3.

terns of hole ordering for the a -axis and respective curves $V(r)$ of potential versus coordinate, where r is the coordinate along the a -axis. The difference between potentials at points 1 and 2 or at 1' and 2' on the AA cross section in Fig. 6 leads to the energy gap E_g shown in Fig. 5. Owing to the equivalence between the two CDWs, the potentials at points 1 and 1' are equal and the ground-state energies of holes approximately equal the minimum potential and are denoted by E_h . The curves of potential with the degeneracy lifted by the crystal field are given in Fig. 6c. In this case the energy difference W between the two minima at points 1 and 1' in Fig. 6c is considerably smaller than E_g . The gap width W for localized holes jumping between neighboring apical bonds is controlled by the local deformation and polarization of lattice. As a result, $W \ll E_g$. The parameter W should be of the order of the phonon energy on the Brillouin zone boundary, $W \approx \hbar \omega_{\text{ph}}(|G|/2)$. Here G is the reciprocal lattice vector along a given crystal axis. Excitations across this gap correspond to local jumps of heavy holes from the lower to upper level (in Fig. 6c from point 1 to point 1'). The deformation of lattice without degeneracy is not shown in Fig. 6c.

Note that energy levels in the potential wells around points 1 and 1' in Fig. 6 are broadened because of the crystal translational symmetry and tunneling between wells, i.e., minibands are formed. The density of states in these bands corresponding to the ground (point 1) and excited (point 1') states of heavy holes is shown in Fig. 5 as two narrow peaks with an energy difference W . The frequency W/\hbar of heavy hole jumps across this gap W may be compared to the resonance frequency in the HTSC electron spectrum proposed by some authors.³²⁻³⁴

4. DISCUSSION

1. The proposed model accounts for some anomalous properties of BKBO, such as negative thermal expansion, upward curvature of the $H_{c2}(T)$ curve, insulator-metal phase transition, etc. In Figs. 6a and 6b the minima of $V(r)$ at points 1 and 1' have equal energies because the two hole localization modes are equivalent. Hence the second-order perturbation term taking into account phonon-assisted

umklapp processes with phonons with $\omega_{\text{ph}}(Q)$ and wave vectors $Q \sim G/2$ on the Brillouin zone boundary is negative. This corresponds to a negative dielectric function $\varepsilon(\omega, q, q+Q)$ at frequencies and wave vectors Q near the Brillouin zone boundary. This means that generation of such phonon should lead to lattice compression, i.e., a negative thermal expansion coefficient. At the same time, generation of other phonons with parameters at which $\varepsilon(\omega, q, q') > 1$ results in lattice expansion. Such phonons stabilize the lattice. For simplicity, we have considered only phonons with wave vectors aligned with one axis.

We can see that in BKBO for $x \leq 0.3$ there is a temperature range $T \lesssim 30$ K in which the mentioned anomalous phonons prevail, i.e., the density of states of such phonons near the Brillouin zone boundary is large.

2. The presence of excitations across the gap W due to the lifting of the degeneracy between the two CDWs (Fig. 6c) is equivalent to a certain boson field. These bosons are short-wave because they correspond to phonon-assisted jumps (tunnelling) of heavy holes between neighboring oxygen ions (to be exact, between Bi–O bonds) at a phonon wave vector $Q \sim G/2$. Thus, a local boson field exists in a BKBO crystal. Interaction of free carriers produced by potassium doping of BKBO should lead to their coupling with a small coherence length ξ . Thus emerges a superconducting state of free carriers with a critical temperature $T_c \sim (W/k) \exp(-1/\lambda)$. The parameter W should be much smaller than the insulating gap $E_g \approx 1-2$ eV and no less than the phonon energy on the Brillouin zone boundary (60–80 meV), i.e., $W \sim 0.1$ eV. In Fig. 5 the gap W is the energy difference between the ground and excited states of heavy holes. The states of light carriers due to potassium doping forming Cooper pairs through interaction with local bosons with the energy W are located near E_F in Fig. 5.

The value of W given above may lead to a critical temperature $T_c \sim 100$ K even when the interaction constant $\lambda = 0.3-0.4$. The estimate $W \leq 0.1$ eV corresponds to peaks in the density of states in a range of 60–80 meV detected by neutron scattering.^{23,35,36} At the same time, experimental data cannot be interpreted in terms of conventional models. Indeed, in the BKBO metallic phase, the Debye temperature Θ increases by more than 30% as the potassium content rises from 0.4 to 0.5.³⁷ It follows from common considerations that the concentration of free carriers and their density of states on the Fermi level should also increase with x in this region. Nonetheless, the measured critical temperature drops by a factor of more than two in this range that contradicts the conventional theory, in which $T_c \sim \Theta \exp(-1/\lambda)$. In the proposed model, the parameter W in the conducting phase drops with the potassium content because of the more efficient Coulomb potential screening by free carriers (Fig. 5). This should lead to a drop in T_c . An accurate theory of the structural transition effect on T_c is given in Ref. 38.

3. In our model, the BKBO superconductivity is largely a consequence of interaction between free carriers and the high-frequency local vibration mode. Given the short wave length of this mode responsible for coupling of carriers in BKBO, the resulting superconducting state has a small coherence length ξ . If a boson-mediated interaction is short-

range, the mean-field approximation is not valid, and the role of order-parameter fluctuations is important, the curve of $H_{c2}(T)$ is anomalous with an upward curvature at all temperatures.³⁹⁻⁴¹ This conclusion is independent of the nature of electron coupling.⁴²

The anomalous shape of the $H_{c2}(T)$ curve with an upward curvature at a field of up to 32 T (Fig. 1) in BKBO and $\lambda \leq 1$ derived from experimental data indicate that the coherence length is small and the interaction leading to superconducting pairing in this material is short-range. Similar anomalous curves were recorded in other HTSC materials with a moderate doping level in which measurements were performed in a wide temperature range.^{43,44} An estimate of the coherence length in BKBO derived from experimental data¹ yields $\xi < 40$ Å.

Note that in BKBO for $x \geq 0.5$, i.e., at a high doping level, the $H_{c2}(T)$ curve is no longer anomalous and can be described in terms of the BCS theory.³⁷ No anomalies in other BKBO parameters were detected in this case. For example, the thermal expansion coefficient α is positive throughout the studied temperature range (Fig. 2).

4. The width of the superconducting gap Δ and the ratio $2\Delta/kT_c$ in BKBO were derived from both tunneling^{45,46} ($2\Delta/kT_c = 3.5-4.1$) and optical^{47,48} ($2\Delta/kT_c = 4.0-4.2$) measurements. These results indicate that BKBO is a superconductor with an intermediate coupling constant. The coupling constant λ derived from the factor γ in the term linear in T of the specific heat versus temperature equals approximately unity, whereas the coupling constant λ_{tr} derived from the formula $\hbar/\tau = 2\pi kT\lambda_{\text{tr}}$ (Ref. 49) using measurements of the BKBO resistivity versus temperature^{50,51} (as well as in other HTSC materials) is only several tenths. Indeed, given the room-temperature resistivity of 230–240 $\mu\Omega \cdot \text{cm}$ ^{50,51} and the carrier concentration $N \approx 3 \cdot 10^{21} \text{ cm}^{-3}$ (Ref. 52), one can easily find $\lambda_{\text{tr}} = 0.3-0.4$. Thus there is an apparent discrepancy between λ derived from thermodynamic and transport measurements. It seems that the thermodynamic λ is overestimated.

Our model accounts for this discrepancy. The true value of λ , which controls T_c , falls between the thermodynamic (derived, for example, from specific heat measurements) and transport values (derived from conductivity measurements). The point is that in addition to the contribution by free carriers (γ_e), excited heavy holes also contribute (γ_h) to the coefficient γ at the linear specific heat term. Although the concentration of these holes is relatively small and, probably, their contribution to the specific heat is nonlinear in T , the term γ_h may be large because of the small width of their energy band (in Fig. 5 their band is split by the gap W), i.e., the coefficient at the linear term in $C = \gamma T$ can be approximated as

$$\begin{aligned} \gamma &\sim N_e(E_F)(1 + \lambda) = N_e(E_F)(1 + \lambda_{ep} + \lambda_{eh}) + N_h(E_F) \\ &\approx N_e(E_F)(1 + \lambda_{ep} + \lambda_{eh} + \lambda_h), \end{aligned}$$

where $N_e(E_F)$ is the density of states of free carriers on the Fermi level, $N_h(E_F)$ is the density of states of tunneling heavy holes on the Fermi level, λ_{ep} is the conventional coupling constant due to the electron-phonon interaction, λ_{eh} is

the contribution due to interaction of free carriers with localized heavy holes, $\lambda_h = N_h(E_F)/N_e(E_F)$ is the contribution due to a small overlap between the upper and lower bands of localized holes (Fig. 5b). Thus it would be more correct to call λ the electron-boson interaction constant due to both the conventional electron-phonon interaction and the coupling to short-wave bosons (heavy holes).

Nonetheless, the contribution of heavy holes to electric current is small because of their large effective mass and low mobility, i.e., the total conductivity

$$\sigma = \sigma_e + \sigma_h = \frac{e^2 N_e}{m_e} \tau_e + \frac{e^2 N_h}{m_h} \tau_h \cong \frac{e^2 N_e}{m_e} \tau_e.$$

Here e is the electron charge, σ_e , m_e , N_e , and τ_e are the conductivity, effective mass, concentration, and transport relaxation time of free carriers, respectively, and σ_h , m_h , N_h , and τ_h are similar parameters of heavy holes. Therefore the measured τ , hence λ_{tr} , is largely controlled by τ_e . Heavy holes may affect τ_e because of scattering of free carriers from them, i.e., $\tau_e^{-1} = \tau_{ep}^{-1} + \tau_{eh}^{-1}$, where τ_{ep} is the relaxation time due to electron-phonon scattering, and τ_{eh} is the relaxation time due to electron scattering from localized holes. As a result, the normal transport and superconducting coupling constants may be very different because of the different contribution by heavy holes.

In tunneling experiments at a small electric field intensity, the contribution of heavy holes to the tunneling current is much smaller than that of free carriers. But at a higher voltage V across the junction, when eV is comparable to W , the current-voltage characteristic should be nonlinear because of the greater contribution by heavy holes.

5. SUMMARY

Measurements of thermal expansion of $Ba_{1-x}K_xBiO_3$ compounds at different x , temperature dependence of the upper critical field $H_{c2}(T)$, and other characteristics demonstrate anomalies, which can be hardly accounted for in terms of the conventional BCS model. The proposed model of the BKBO electronic structure can be used to interpret anomalous properties of these compounds. The model is based on the ordering of oxygen atoms with different valences located at two opposite apices of the oxygen octahedron in BKBO or polyhedron in other HTSC. This ordering is equivalent to emergence of CDWs in BKBO and leads to doubling of the lattice cell and a metal-insulator phase transition. The presence of two degenerate CDWs results in a negative dielectric function for wave vectors on the Brillouin zone boundary, hence to negative thermal expansion at low temperatures. Lifting of degeneracy of these two CDWs generates a gap W in the energy spectrum of heavy holes. Excitations across the gap W are short-wave bosons. They correspond to local excitations and local lattice polarization due to tunneling of heavy holes between neighboring Bi-O (or Cu-O) bonds, where O is apical oxygen. The coupling of free carriers via these local virtual bosons leads to a superconductivity with a high T_c . Concurrently, coupling via phonons may also occur. The local nature of bosons leads to a short coherence length ξ , hence the $H_{c2}(T)$ curve has an anomalous upward curva-

ture throughout the studied temperature range. Owing to the localization of holes, which are responsible for short-wave bosons, the coupling constants λ derived from thermodynamic and transport measurements are different. This mechanism of superconductivity after obvious minor modifications can be applied to other high- T_c superconductors.

The work was supported by the Scientific Counsel on the HTSC problem (project No. 93069), International Science Foundation (grant N9V000), and on the final stage by the Russian Fund for Fundamental Research (project No. 95-02-06052a).

- ¹G. Kh. Panova, A. A. Shikov, B. I. Savel'ev *et al.*, Zh. Éksp. Teor. Fiz. **103**, 605 (1993) [JETP **76**, 302 (1993)].
- ²C. Escribe-Filippini, J. Marcus, M. Affronte *et al.*, Physica C **210**, 133 (1993).
- ³M. Affronte, J. Marcus, C. Escribe-Filippini *et al.*, Phys. Rev. B **49**, 3502 (1994).
- ⁴M. Licheron, I. Reynaud, R. P. S. M. Lobo *et al.*, Physica C **235-240**, 709 (1994).
- ⁵L. F. Mattheiss and D. R. Hamann, Phys. Rev. B **28**, 4227 (1983).
- ⁶M. Verwerft, G. Van Tendeloo, D. G. Hinks *et al.*, Phys. Rev. B **44**, 9547 (1991).
- ⁷A. L. Shelehov, N. V. Anshukova, A. I. Golovashkin *et al.*, Physica C **185-189**, 989 (1991).
- ⁸O. V. Ivanov, E. G. Maksimov, I. I. Mazin *et al.*, Sol. St. Commun. **76**, 1267 (1990).
- ⁹M. Licheron, N. Lissart, and F. Gervait, Sol. St. Commun. **79**, 667 (1991).
- ¹⁰Y. J. Uemura, B. J. Sternlieb, D. E. Cox *et al.*, Nature **335**, 151 (1988).
- ¹¹L. N. Bulaevskii and O. V. Dolgov, Pis'ma v Zh. Éksp. Teor. Fiz. **45**, 413 (1987) [JETP Lett. **45**, 526 (1987)].
- ¹²B. Batlogg, R. J. Cava, L. F. Schneemeyer, and G. P. Espinosa, IBM J. Research and Development **33**, 208 (1989).
- ¹³N. V. Anshukova, Yu. V. Boguslavskii, A. I. Golovashkin *et al.*, Fiz. Tverd. Tela **35**, 1415 (1993) [Phys. Solid State **35**, 714 (1993)].
- ¹⁴N. V. Anshukova, A. I. Golovashkin, L. I. Ivanova, and A. P. Rusakov, in *Progress in High Temperature Superconductivity* (Proceedings of Intern. Conf. on HTSC and Localization Phenomena) **32**, 403 (1991).
- ¹⁵N. V. Anshukova, A. I. Golovashkin, L. I. Ivanova, and A. P. Rusakov, Sverkhprovodimost': Fiz., Khim., Tekh. **5**, 644 (1992).
- ¹⁶N. V. Anshukova, A. I. Golovashkin, L. I. Ivanova, and A. P. Rusakov, J. Supercond. **7**, 423 (1994).
- ¹⁷A. I. Golovashkin, N. V. Anshukova, L. I. Ivanova, and A. P. Rusakov, Physica C **235-240**, 1299 (1994).
- ¹⁸N. V. Anshukova, V. B. Ginodman, A. I. Golovashkin *et al.*, Zh. Éksp. Teor. Fiz. **97**, 1635 (1990) [Sov. Phys. JETP **70**, 923 (1990)].
- ¹⁹N. V. Anshukova, A. I. Golovashkin, L. I. Ivanova *et al.*, Sverkhprovodimost': Fiz., Khim., Tekh. **7**, 1573 (1994).
- ²⁰S. Pei, J. D. Jorgensen, B. Dabrowsky *et al.*, Phys. Rev. B **41**, 4126 (1990).
- ²¹M. L. Norton, Mater. Res. Bull. **24**, 1391 (1989).
- ²²J. M. Rosamilia, S. H. Glarum, R. J. Cava *et al.*, Physica C **182**, 285 (1991).
- ²³M. G. Zemlyanov, P. P. Parshin, P. I. Soldatov *et al.*, Sverkhprovodimost': Fiz., Khim., Tekh. **4**, 961 (1991).
- ²⁴N. V. Anshukova, A. I. Golovashkin, V. S. Gorelik *et al.*, J. Mol. Struct. **219**, 147 (1990).
- ²⁵E. Helfand, N. R. Werthamer, and P. C. Hohenberg, Phys. Rev. **147**, 295 (1966).
- ²⁶Z. X. Shen, P. A. P. Lindberg, B. O. Wells *et al.*, Phys. Rev. B **40**, 6912 (1989).
- ²⁷S. M. Heald, D. DeMarsio, M. Croft *et al.*, Phys. Rev. B **40**, 8828 (1989).
- ²⁸S. H. Blanton, R. T. Collins, K. H. Kelleher *et al.*, Phys. Rev. B **47**, 996 (1993).
- ²⁹M. A. Karlow, S. L. Cooper, A. L. Kotz *et al.*, Phys. Rev. B **48**, 6499 (1993).
- ³⁰S. K. Sinha, D. Vaknin, M. S. Alvarez *et al.*, Physica B **156-157**, 854 (1989).
- ³¹N. Nagoshi, Y. Fukuda, T. Suzuki *et al.*, Physica C **185-189**, 1051 (1991).
- ³²R. S. Markiewicz, Intern. J. Mod. Phys. B **5**, 2037 (1991).
- ³³E. K. Naimi, Phys. Stat. Sol. (b) **177**, 213 (1993).

- ³⁴A. A. Gorbatshevich, Yu. V. Kopaev, and I. V. Tokatly, *Physica C* **233**, 95 (1994).
- ³⁵C. K. Loong, P. Vashishta, R. K. Kalia *et al.*, *Phys. Rev. B* **45**, 8052 (1992).
- ³⁶D. G. Hinks, B. Dabrowski, D. R. Richards *et al.*, *Mat. Res. Soc. Symp. Proc.* **156**, 357 (1989).
- ³⁷M. N. Khlopkin, G. H. Panova, A. V. Suetin *et al.*, *Sverkhprovodimost': Fiz., Khim., Tekh.* **7**, 495 (1994).
- ³⁸Yu. V. Kopaev, *Trudy FIAN* **86**, 3 (1975).
- ³⁹R. Micnas, J. Ranninger, and S. Robaszkiewicz, *Rev. Mod. Phys.* **62**, 113 (1990).
- ⁴⁰S. Ullach and A. T. Dorsey, *Phys. Rev. B* **44**, 262 (1991).
- ⁴¹A. S. Aleksandrov and A. B. Krebs, *Usp. Fiz. Nauk* **162**, 1 (1992).
- ⁴²A. S. Alexandrov and J. Ranninger, *Sol. St. Commun.* **81**, 403 (1992).
- ⁴³A. P. Mackenzie, S. R. Julian, G. G. Lonzarich *et al.*, *Phys. Rev. Lett.* **71**, 1238 (1993).
- ⁴⁴M. S. Osofsky, R. J. Soulen, S. A. Wolf *et al.*, *Phys. Rev. Lett.* **71**, 2315 (1993).
- ⁴⁵B. A. Baumert and J. Talvacchio, *IEEE Trans. Appl. Supercond.* **3**, 1567 (1993).
- ⁴⁶M. Kosugi, J. Akimitsu, T. Uchida *et al.*, *Physica C* **229**, 389 (1994).
- ⁴⁷F. J. Dunmore, H. D. Drew, E. J. Nicol *et al.*, *Phys. Rev. B* **50**, 643 (1994).
- ⁴⁸A. V. Puchkov, T. Timusk, W. D. Mosley, and R. N. Shelton, *Phys. Rev. B* **50**, 4144 (1994).
- ⁴⁹M. J. G. Lee, *Phys. Rev. B* **2**, 250 (1970).
- ⁵⁰H. Sato, T. Ido, S. Tajima *et al.*, *Physica C* **185-189**, 1343 (1991).
- ⁵¹M. Iyori, S. Suzuki, H. Suzuki *et al.*, *Jap. J. Appl. Phys.* **32**, 1946 (1993).
- ⁵²S. Guha, D. Peebles, V. Browning *et al.*, *J. Supercond.* **6**, 339 (1993).

Translation was provided by the Russian Editorial office.